Biomass Conversion and Biorefinery
https://doi.org/10.1007/s13399-024-05432-5

ORIGINAL ARTICLE

The effect of impregnation ratio and surface modification on the characteristics and performance of activated carbon derived from *Ficus carica* leaves for Cr(VI) removal

Zohra Baassou[1] · Fatiha Benmahdi[2] · Abdelbaki Reffas[1] · Abdelhamid Benhaya[3]

Received: 4 December 2023 / Revised: 7 February 2024 / Accepted: 10 February 2024

Abstract
Hexavalent chromium (Cr(VI)) is a water-soluble, highly toxic form of chromium compound that is recognized as a carcinogen and can lead to various health issues. This research investigates the use of activated carbon (AC) derived from *Ficus carica* leaves for the removal of Cr(VI) from water. The effect of the impregnation ratio on the characterization and performance of activated carbons for removing Cr(VI) was investigated. The physicochemical and textural properties of the produced activated carbons (ACs) were characterized using various analyses, including XRD, SEM, TGA, FTIR, iodine number, and pH of zero charge. It was found that the AC-100 impregnated at a ratio (AC/H_3PO_4) of 100% indicated highly efficient removal of Cr(VI). The prepared ACs have been modified with ethylenediamine (EDA) to enhance their performance. Results show that the adsorption capacity of the modified ACs showed a significant enhancement in comparison to the raw ACs. The maximum adsorption capacities for Cr(VI) removal for the raw AC-100 and its modified form were found to be 155.22 and 203.25 mg/g, respectively, as determined by the Langmuir isotherm. The results of this study confirm that EDA can be used to enhance the effectiveness of activated carbon (AC) derived from *Ficus carica* leaves in removing Cr(VI) from water.

Keywords Modified activated carbon · Chemical activation · *Ficus carica* leaves · Adsorption equilibrium · Chromium hexavalent · Ethylenediamine

1 Introduction

The rapid expansion of industry activity has resulted in the contamination of the aquatic environment with a wide array of toxic and hazardous chemicals [1–3]. Effective wastewater management and treatment are crucial to mitigate the environmental impact of these pollutant sources and to ensure safe water disposal and conservation. Addressing this issue requires innovative approaches, and recent research has made significant contributions in the field of pollutant detection and removal [4, 5]. Among these pollutants, heavy metals stand out as highly perilous inorganic contaminants, even when present in low concentrations in aqueous solutions [6]. These metals have long half-lives and cannot be degraded [7]. Chromium is found in two forms: trivalent Cr(III) and hexavalent Cr(VI) chromium. Hexavalent Cr(VI) is particularly pernicious due to its elevated oxidation potential and remarkable transmembrane mobility, classifying it as a Group I carcinogen [8]. The World Health Organization (WHO) has established stringent guidelines, specifying limits of 0.05 mg/L for Cr(VI) in drinking water and 0.1 mg/L for surface water [9].

Chromium sources in wastewater are diverse and can originate from various industrial, municipal, and natural origins. Industries such as metal plating, tanneries, and chemical manufacturing contribute significant amounts of chromium through their processes [10]. Municipal sewage also contains chromium from domestic sources, like household products. Natural sources, such as geological deposits

✉ Fatiha Benmahdi
fatiha.benmahdi@univ-batna.dz

[1] Inorganic Materials Laboratory, LMI, Department of Chemistry, Faculty of Science, University of Mohamed Boudiaf, 28000 M'sila, Algeria

[2] Laboratory of Chemistry and Environmental Chemistry (LCEE), Department of Chemistry, Faculty of Matter Sciences, Route de Biskra, University of Batna1, 05000 Batna, Algeria

[3] Advanced Electronic Laboratory, Department of Electronics, Mostapha Benboulaid Batna 2 University, 05000 Batna, Algeria

Published online: 21 February 2024

and atmospheric deposition, can introduce trace amounts of chromium into wastewater.

Methods including coagulation/flocculation [11], precipitation [12], adsorption [13], ion exchange [14], reverse osmosis [15], and membrane filtration [16] are employed to remove Cr(VI) from wastewater. The adsorption process has been identified as the most efficient and environmentally sustainable method [17]. The ability to regenerate the adsorbents when necessary is another benefit [8]. The use of various adsorbents for wastewater purification, such as bentonite [18], mesoporous silica [19], humic acid-derived resin [20], nanoadsorbent [21] composite materials [22, 23], nanocomposite [24], biosorbents [25, 26], and activated carbons [27, 28], has been the subject of extensive research in recent years.

Activated carbon (AC) emerges as a remarkably significant material with diverse applications across various fields, including energy storage [29–31], and wastewater treatment. Its prominence is attributed to factors such as large surface area, cost-effectiveness, high reactivity, and minimal negative environmental impact [32, 33], have considerable in the removal of hexavalent chromium from water [34, 35]. Moreover, the exploration of enhancing activated carbon (AC) through surface modification with various chemicals, including acids, basic materials, and polymers, adds an intriguing dimension due to its potential to boost AC efficiency [36, 37].

Through a series of procedures, activated carbon can be created from any source material with a high carbon concentration [38]. These procedures transform carbonaceous materials into a highly porous and adsorptive substance. According to Liang et al. [39], wood is the most widely used raw material for the production of activated carbon [40], followed by agricultural wastes. Various forms of agricultural waste, including seeds [41, 42], leaves [43, 44], peels [45, 46], and stems [47], coffee-derived biowaste [48], sawdust [49], and corncob [50, 51], have been harnessed for the production of AC. This study focuses specifically on the utilization of leaves as a biomass source for AC production. The significance of leaves as valuable precursors in material production is underscored by a variety of studies that explore their distinctive properties and applications [52–55].

Carbonization and activation are the two key stages involved in the manufacture of activated carbon. The first stage entails heating carbonaceous materials beyond 600 °C without oxygen in order to transform them into solid carbon products [56]. The technique of applying physical activation or chemical activation to increase the porosity and surface area of activated carbon is the second phase. Physical activation is a less effective, but more expensive, way to create activated carbon than chemical activation. Typically, chemical activation is employed to produce activated carbon with large pore volumes and surface areas [57, 58].

The impregnation of a raw material with an activating agent and subsequent heating to a high temperature constitute the chemical activation process. By creating holes in the raw material by an activating agent reaction, the surface area and adsorption capacity are increased. Potassium hydroxide (KOH), sodium hydroxide (NaOH), zinc chloride ($ZnCl_2$), and phosphoric acid (H_3PO_4) are the most often utilized activating agents. The final one has a variety of benefits over other chemical agents, including high efficiency, a non-corrosive acid, relative environmental friendliness, ease of use, and affordability. It creates activated carbon with a variety of pore sizes and high surface areas [59, 60].

The objective of this study focuses on the chemical activation of an agricultural waste, *Ficus carica* leaves, utilizing H_3PO_4 as an activating agent for a range of impregnation ratios (30, 60, 100, 150, and 200%) to produce activated carbon. By using XRD, SEM, TGA, FTIR, iodine number, methylene blue (MB) index, pH_{PZC}, and Boehm titration, the prepared ACs were characterized. Using batch adsorption process, the prepared ACs were employed to remove Cr(VI) from an aqueous media. It was investigated how different parameters, including adsorbent dosage, solution pH, Cr(VI) concentration, and contact time, affected the adsorption process. Ethylenediamine (EDA) has been used to modify the prepared ACs surfaces in order to improve their performance. Also, the equilibrium adsorption isotherms of Cr(VI) on unmodified and EDA-modified ACs were investigated.

2 Materials and methods

2.1 Materials

The following chemicals were supplied by Sigma-Aldrich, Algeria: $K_2Cr_2O_7$ (99.5%), H_3PO_4 (85%), 1,5-diphenylcarbazide (99%), ethylenediamine ($C_2H_8N_2$) (≥ 99%), KI (99%), I_2 (99%), NaOH (98%), H_2SO_4 (98%), HCl (36.5–38%), and acetone (99%). In order to make the Cr(VI) stock solution (1 g/L), 2.83 g of $K_2Cr_2O_7$ and 1L of distilled water were used.

2.2 Activated carbon preparation

Ficus carica leaves were collected in the local region in eastern Algeria. The leaves were cleaned with distilled water to get rid of any pollutants before being dried outside for a couple of days. In order to obtain particles with a diameter of less than 900 m, the acquired precursor was crushed and sieved. A chemical activation was carried out by the socking of 60 g of the precursor with a desired amount of H_3PO_4 (30, 60, 100, 150, 200 wt %) in an ultrasound probe (BRANSON 2510) for 2 h. The mixture was heated to 600 °C for 1.5 h in a turbulent

muffle furnace (LINDBERG 54576-S HEVI-DUTY) with a heating rate of 15 °C min^{-1} after being evaporated at 105 °C in an oven. The resulting sample was rinsed several times with hot distilled water to remove excess phosphoric acid. After drying at 105 °C for 24 h, crushing, and sieving the activated carbon (AC) to a diameter of less than 75 µm, the activated carbon (AC) noted is ready for use. The prepared ACs were given the labels AC-30, AC-60, AC-100, AC-150, and AC-200 in accordance with their impregnation ratios. Ethylenediamine (EDA) has been added to the produced ACs to improve their adsorption abilities. To achieve this, 2 mL of ethylenediamine was gradually added to a mixture of 300 mg of AC and 50 mL of distilled water in an ultrasound probe (BRANSON 2510) at 40 °C for 2 h. The resultant sample was then dried after being rinsed with ethanol and water in a 1:1 ratio and filtered using a 0.45-µm filter. The label for the modified activated carbon read EDA-AC.

2.3 Characterizations

The elemental composition and surface appearance of the AC were characterized using scanning electron microscopy (SEM). A spinning Cu K anode (1.54060) was used in an X-ray diffractometer (XRD; Rigaku MiniFlex600) investigation to ascertain the composition of AC. Shimadzu's DTG-60 thermogravimeter was used to analyze the thermogravimetry of ACs between 25 and 1000 °C (10 °C/min). Based on FTIR spectra collected with a Perkin Elmer Two FTIR spectrophotometer from Perkin Elmer, USA, the chemical functional groups of the ACs were identified. The ACs were examined as prepared KBr pellets with 20 scans between 4000 and 400 cm^{-1} and a resolution of 4 cm^{-1}. Additionally, the Boehm titration method (Boehm, 1966) was used to calculate the amount of chemical functional groups present on the surface of AC [61].

The point of zero charge (pH_{PZC}) of AC was determined using a batch technique [62]. In a series of Erlenmeyer flasks containing 50 mL of NaCl solution (0.1 mol/L), a mass of 0.2 g of AC was added to each flask, and the mixture was stirred for 48 h at room temperature. The pH was varied from 2 to 10 by added HCl (0.1 mol/L) and NaOH (0.1 mol/L) to the pH noted pH_i. The curve of pH as a function of pH_i was used to determine pH_{PZC}. The pH at the point where the surface charge of the activated carbon is zero represents pH_{pzc} [63]

The adsorption performance of the produced ACs was assessed by measuring the methylene blue and iodine numbers. Iodine number was determined using the experimental protocol proposed by ASTM [64]. A mass of 0.1 g of AC is placed in a clean bottle in contact with 10 mL of 5% HCL and allowed to boil for 30 s. Then, 100 mL of iodine solution (0.1 N) was added to the mixture, which was agitated for 30 s, and the mixture was quickly filtered on filter paper. A volume of 10 mL of the filtrate is dosed by a sodium thiosulfate solution of 0.1 N in the presence of starch as an ending indicator. Methylene blue (MB) index was determined according to the Chemviron-Carbon Company (Zoning Industriel C. B-7181 Feluy, Belgium) TM-1 standard test method [28]. In an Erlenmeyer flask containing 0.1 g AC, a standard MB solution (1500 mg/L) is added in small volumes, and the mixture is shaken for a few minutes. Once equilibrium is reached and the AC is saturated with MB, a very light blue color appears with the last amount of MB added just before reaching equilibrium. The total volume (V_{MB}) adsorbed is then calculated, and the MB index, expressed in terms of milligrams of MB adsorbed per gram of activated carbon, is determined using Eq. 1.

$$\text{MB index} = \frac{1500 \times V_{MB}}{0.1} \tag{1}$$

2.4 Adsorption study

Adsorption study carried out using a batch process, a predetermined volume of the Cr(VI) solution was combined with a certain mass of AC in a reactor and agitated until equilibrium. The mixture was centrifuged at 4000 rpm for 20 min after equilibrium was reached, and the filtrate was then combined with 1,5-diphenylcarbazide and examined using a UV spectrophotometer at 554 nm. Investigation was done into the effects of various operating parameters, including the AC dose, solution pH, time, and beginning Cr(VI) content. Furthermore, the equilibrium adsorption was investigated under the optimum conditions. The adsorption capacity of Cr(VI) at equilibrium, q_e, and at time t, q_t, were calculated from Eq. 2 and Eq. 3, respectively.

In a batch-processed adsorption investigation, the equilibrium adsorption was examined under optimal operating conditions. Equation 2 and Eq. 3 were used to calculate the adsorption capacity of Cr(VI) at equilibrium, q_e, and at time t, q_t, respectively [65, 66].

$$q_e(\text{mg/g}) = \frac{(C_0 - C_e)(\text{mg/L})}{m_{AC}(\text{g})} V(\text{L}) \tag{2}$$

$$q_t(\text{mg/g}) = \frac{(C_0 - C_t)(\text{mg/L})}{m_{AC}(\text{g})} V(\text{L}) \tag{3}$$

3 Results and discussion

3.1 Characteristics of the prepared ACs

The X-ray diffraction (XRD) patterns of the ACs that were prepared are presented in Fig. 1. As shown in this analysis, the produced ACs exhibit a similar structure across various impregnation ratios. The prominent and wide peaks

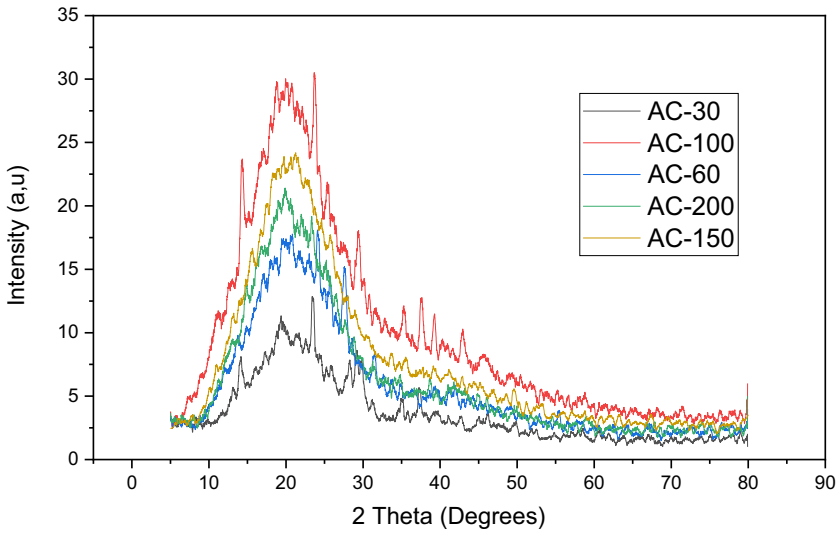

Fig. 1 The XRD diagrams of the prepared activated carbons

appearing between 20 and 35° can be attributed to graphite disorder, as reported by [67]. Furthermore, a minor peak observed between 40 and 50° may be associated with the stacking arrangement of aromatic carbon layers. Similar findings for various prepared AC types have been reported in numerous research [68–70] as well as for commercial AC [71]. According to [72], the peaks at about 24° and 43° correspond to, respectively, the (0 0 2) planes of disorder aromatic carbon and the (0 0 1) planes of graphite's hexagonal structure, showing the predominance of an amorphous structure.

Scanning electron microscopy (SEM) analysis of the surface morphologies of the produced ACs, shown in Fig. 2, reveals a different pattern. Notably, these ACs have a rough surface structure and uneven porosity. The apparent porosity supports the successful pyrolysis and activation procedure that was accomplished by utilizing phosphoric acid.

The thermogravimetric analysis (TGA) results for all the prepared ACs demonstrate a two-stage weight loss pattern, as illustrated in Fig. 3. The release of adsorbed water is thought to be responsible for the initial stage, which occurs up to 250 °C. The next stage involves the thermal breakdown of oxygen functional groups and occurs between 300 and 800 °C. Other researchers [42, 58] for a variety of prepared activated carbons have reported similar findings.

The FTIR spectra of the prepared ACs (Fig. 4) have consistent structural features with distinct bands. The broad band observed at 3425 cm^{-1} can be attributed to the presence of free hydroxyl groups (O–H) on the surface of the ACs, as reported by [73, 74]. Furthermore, the absorption peaks at 2923.92 cm^{-1}, 1620 cm^{-1}, and 1097 cm^{-1} may be due to -CH_2 groups (methyl and methylene groups) [75], C = C bonds [76], and C-O stretching vibration in carboxylic acids, alcohols, phenols, and esters, respectively. The peaks falling within the 612–779 cm^{-1} range can be attributed to the interaction of phosphorous species resulting from the phosphoric acid activation process, as suggested by [77].

The results of the Boehm titration analysis of the prepared CAs are illustrated in Fig. 5. It is clear that the prepared ACs contain more acidic than basic groups, with lactonic and phenolic groups making up the majority of the acidic groups. The point of zero charge (pH_{PZC}) values in Fig. 6, which vary from 5.44 to 5.61, support the conclusion that the prepared ACs are mildly acidic. Table 1 lists additional properties for all prepared ACs, including the iodine number, methylene blue (MB) index, yield, apparent density, slurry pH, humidity, porosity, and pH_{PZC}.

The iodine number values obtained for the prepared ACs exhibit a notable range, spanning from 1117 to 1346 mg/g. As can be observed in Table 1, the iodine number rises as a result of the phosphoric acid impregnation ratio. These high iodine numbers show that the activation process has produced desirable microporosity and that the activated carbon that has been formed has a sizable microporous surface area [78]. According to the literature, the iodine number values expected for high-quality activated carbons are equal to or higher than 900 mg/g. Moreover, the literature provides a broader context by specifying a typical iodine number range of 500–1200 mg/g, equivalent to a surface area range of 900–1100 m^2/g [79]. This suggests that the prepared activated carbons exhibit a surface area that exceeds the typical expectations, further emphasizing their potential for efficient adsorption. In addition, the low-density values validate the porous structure of the ACs and confirm the existence of a large specific surface area [80]. The MB index values ranged from 35.82 to 46.8 mg/g, demonstrating that chemical

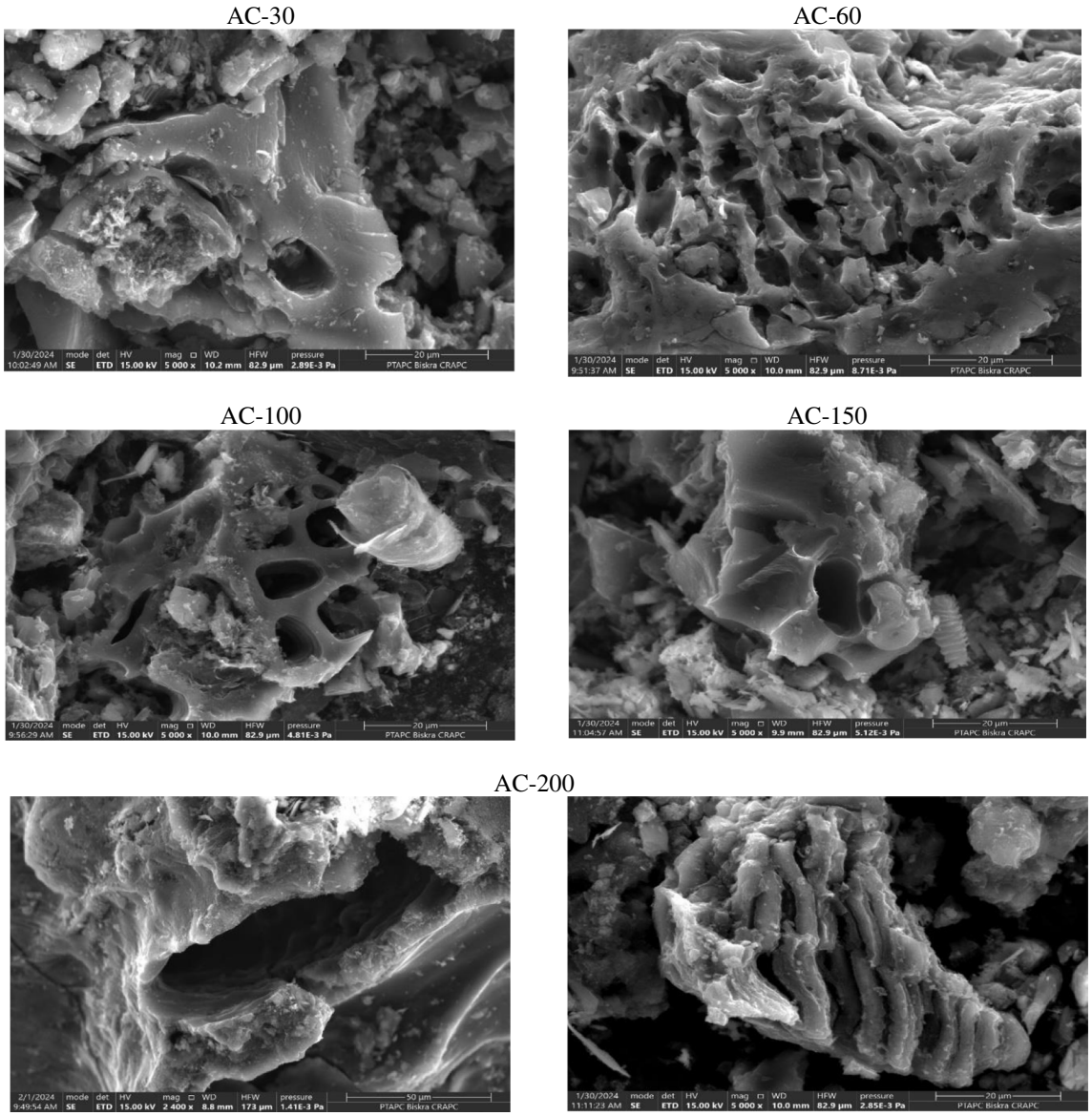

Fig. 2 SEM analysis of the prepared activated carbons

activation with phosphoric acid had a detrimental effect on the development of mesoporous surface area. This shows that the structure of the prepared ACs is largely microporous. These ACs can also be used to remove substances with tiny diameters, such as hexavalent chromium.

3.2 Adsorption study

3.2.1 Effect of parameters on adsorption of Cr(VI)

The effect of pH (2–12) on the removal of Cr(VI) using the prepared ACs is presented in Fig. 7. The highest Cr(VI) removal efficiency was accomplished at very low pH, with removal yields ranging from 98.18 to 75.83% at pH 2–4. This finding is in line with earlier studies [35, 81]. This is due to the anionic form of chromium, $HCrO_4^-$, which predominates in low pH solutions and is drawn to the positively charged surfaces of the ACs. The prepared ACs all have an acidic point of zero charge (pH_{PZC}), which indicates that at pH levels below their pH_{PZC}, their surfaces are positively charged. For additional research, pH 2 was kept constant.

The effect of the AC dose on the adsorption of Cr(VI) is illustrated in Fig. 8. It is evident that with an increase in the amount of AC, the adsorption efficiency also increases, which is due to the availability of more adsorption sites on the surface of AC. All activated carbons exhibit comparable behavior, with only slight variation in their removal efficiency. The optimal ACs dose for the effective removal

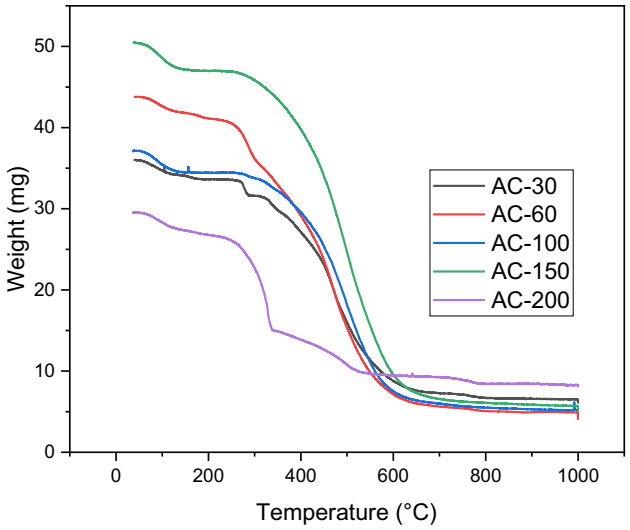

Fig. 3 ATG analysis curves of the prepared ACs

of Cr(VI) was determined to be 2 g/L, achieving a removal efficiency of 98%. This dose was subsequently maintained constant for further study.

The effect of contact time on the removal of Cr(VI) was investigated using the prepared activated carbons (ACs) at an initial concentration of 100 mg/L, as depicted in Fig. 9. The results reveal a clear trend, wherein an extension of the contact time results in a corresponding increase in the removal efficiency of Cr(VI). This phenomenon can be attributed to the prolonged contact time facilitating the diffusion of Cr(VI) onto the microporous surface of the ACs, allowing it to effectively bind to available adsorption sites. Equilibrium in the adsorption process is observed to be achieved at approximately 2 h of contact time, and this duration was subsequently adopted as the equilibrium contact time for further study.

3.2.2 Equilibrium adsorption isotherms

The equilibrium adsorption isotherms of all prepared ACs were investigated in the range of initial Cr(VI) concentration spanning from 50 to 450 mg/L, under optimal operational conditions (ACs dose of 2 g/L, pH of 2, a contact time of 2 h, and ambient temperature). The resulting isotherms are illustrated in Fig. 10. It is evident that the adsorption capacity for Cr(VI) rises with increasing residual Cr(VI) concentrations at equilibrium, reaffirming the favorable adsorption characteristics of Cr(VI) on all the prepared ACs, albeit with slight variations in equilibrium capacity among the different AC samples.

Two adsorption isotherm models, namely the Freundlich model (Eq. 4) proposed by [82] and the Langmuir model (Eq. 5) introduced by [83], were employed to assess the Cr(VI) adsorption parameters (Fig. 11).

$$q_e = K_F C_e^{1/n} \tag{4}$$

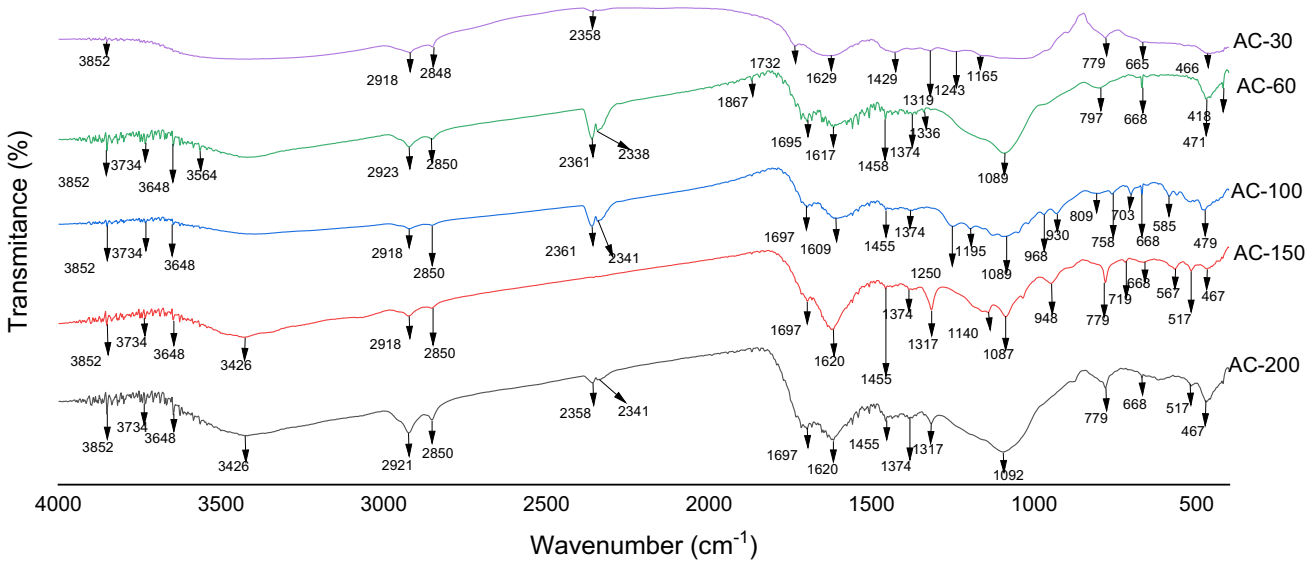

Fig. 4 FTIR spectra of the prepared ACs

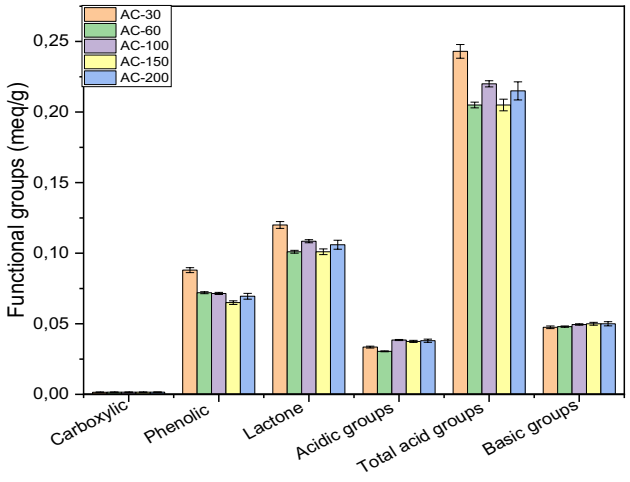

Fig. 5 Functional groups of the prepared CAs

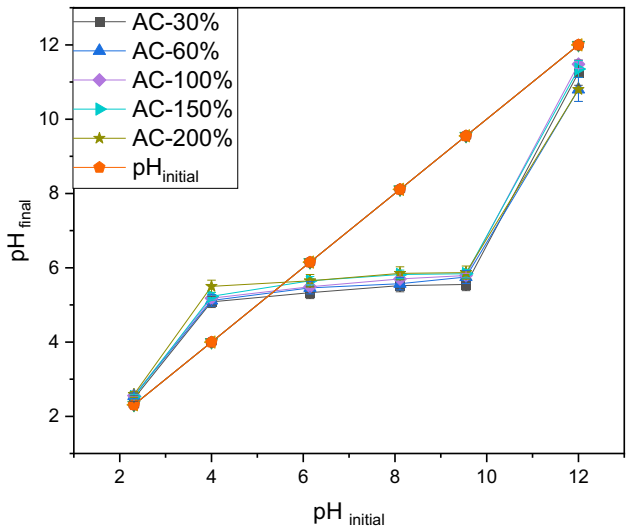

Fig. 6 The pH_{PZC} of the prepared ACs

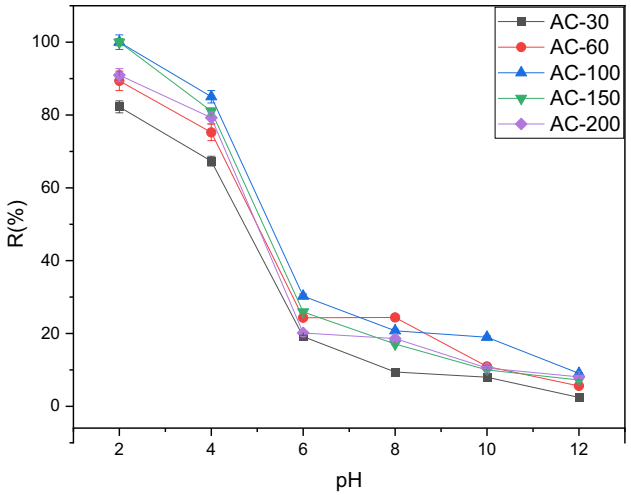

Fig. 7 The effect of pH on the adsorption of Cr(VI) in the prepared ACs (time = 2 h, ambient temperature, an initial Cr(VI) concentration = 100 mg/L)

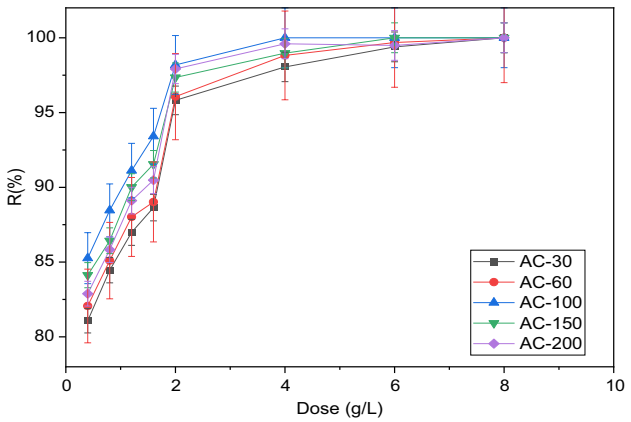

Fig. 8 The effect of ACs dose on the adsorption of Cr(VI) (pH = 2, time = 2 h, ambient temperature, an initial Cr(VI) concentration = 100 mg/L)

Table 1 Physicochemical characteristics of the prepared ACs

Parameters	Adsorbents				
	AC-30	AC-60	AC-100	AC-150	AC-200
Production yield (%)	56.7	52.2	48.6	44.8	42.5
Slurry pH	5.48	4.83	3.73	3.42	3.40
pH_{PZC}	5.44	5.46	5.52	5.60	5.62
Iodine number (mg/g)	1117	1257	1270	1310	1346
BM index	38.92	35.82	46.80	37.25	36.42
Apparent density (g/cm^3)	0.60	0.61	0.62	0.62	0.63
Porosity (ζ) (%)	44.54	44.26	44.51	44.52	44.51
Humidity level (%)	2.71	3.31	4.3	3.59	2.89
Conductivity (μs)	260	266	259	262	257

where q_e (mg/g): the equilibrium adsorption capacity, C_e (mg/L): the equilibrium concentration of Cr(VI), K_F ($mg^{1-(1/n)}\,L^{1/n}\,g^{-1}$): the Freundlich constant, and n: a measure of the adsorption intensity.

$$q_e = \frac{q_m K_L C_e}{1 + K_L C_e} \tag{5}$$

where q_m (mg/g): the maximum adsorption capacity for a monolayer coverage of the AC (mg/g), and K_L (L/mg): the Langmuir constant.

The parameter values for each adsorption isotherm are provided in Table 2. The correlation coefficient (R^2) values reveal that the Langmuir model suitably describes the adsorption data for all ACs. The maximum adsorption

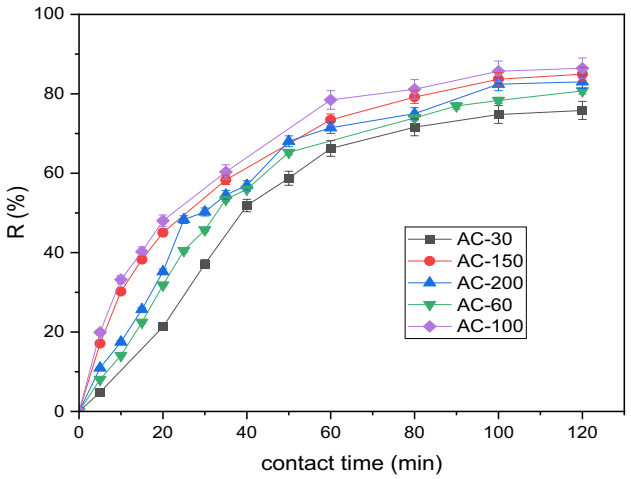

Fig. 9 The effect of contact time on the equilibrium adsorption of Cr(VI) onto the prepared ACs (AC dose = 2 g/L, pH = 2, ambient temperature, an initial Cr(VI) concentration = 100 mg/L)

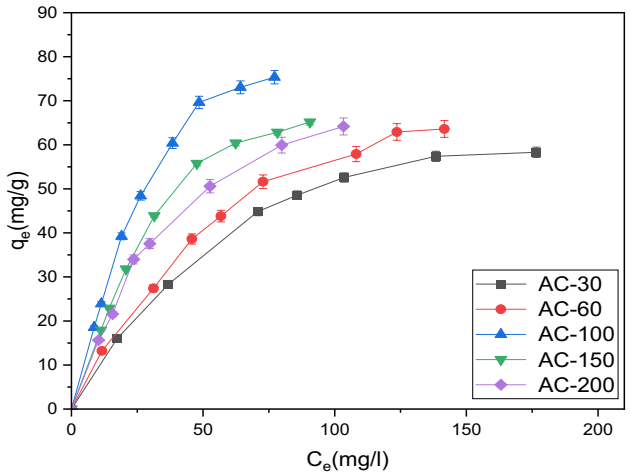

Fig. 10 The adsorption isotherms of Cr(VI) on the prepared ACs (ACs dose of 2 g/L, pH of 2, a contact time of 2 h, and ambient temperature)

increases from 93.28 to 155.27 mg/g as the impregnation ratio increases from 30 to 100%. Subsequently, with a further increment in the impregnation ratio from 100 to 200%, the maximum capacity decreases to 112.86 mg/g. Among the ACs, AC-100 stands out with the highest maximum capacity, signifying the optimal impregnation ratio of the activating agent (H_3PO_4). This result highlights the crucial role of impregnation ratio in modifying the adsorption capacity of activated carbons for Cr(VI) removal.

The maximum adsorption capacity of the selected AC (AC-100) is compared with that of several other prepared ACs used for Cr(VI) removal, as illustrated in Table 3. It can be seen that the prepared AC-100 exhibits a notably greater maximum adsorption capacity in comparison to the majority of previously reported adsorbents, reaffirming its effectiveness for Cr(VI) removal. This AC can be considered a promising adsorbent for the effective removal of Cr(VI) from water.

The effect of the surface modification by EDA Ethylenediamine (EDA) was employed as a surface modification agent to enhance the performance of the prepared ACs for the removal of Cr(VI). In Fig. 12, equilibrium adsorption isotherms for all modified ACs are presented. To determine the adsorption parameters and the most suitable isotherm model, the adsorption data were fitted using the Freundlich and Langmuir isotherms, as shown in Fig. 13. The results in Table 4 affirm that the adsorption of Cr(VI) onto all modified ACs (EDA-ACs) is well-described by the Langmuir isotherm, as indicated by the high correlation coefficient (R^2) values. A comparison of the maximum adsorption capacities of the unmodified ACs and the EDA-ACs confirms a notable enhancement in the performance of the ACs. Specifically, the maximum adsorption capacity increased from 155.27 to 203.25 mg/g for EDA-modified AC-100 (EDA-AC-100).

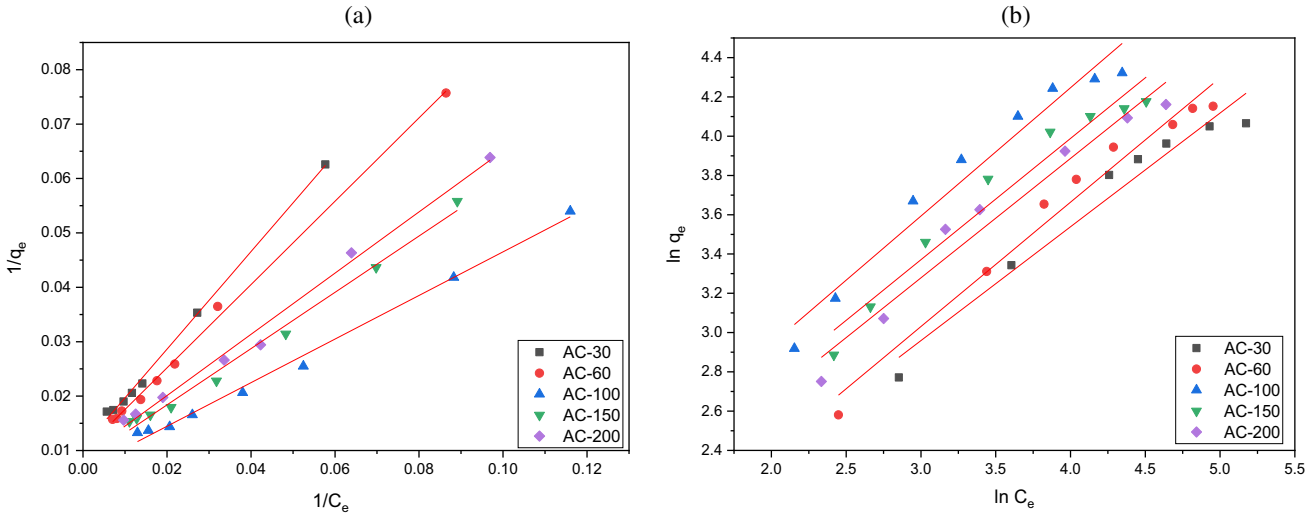

Fig. 11 Linear fit of Langmuir (**a**) and Freundlich (**b**) isotherms models for Cr(VI) removal by the prepared ACs

Table 2 Adsorption isotherm constants for removal of Cr(VI)) using the prepared ACs

Model	Parameters	Adsorbent				
		AC-30	AC-60	AC-100	AC-150	AC-200
Langmuir	q_{max} (mg/g)	93.28	101.31	155.27	124.37	112.86
	K_L (L/mg)	0,011	0.012	0,016	0,0155	0,015
	R_L	0.62	0.608	0.608	0.562	0.559
	R^2	0.997	0.997	0.992	0.990	0.989
Freundlich	$1/n$	0.57	0.633	0.65	0.61	0.60
	K_F ($mg^{1-(1/n)}\ L^{1/n}\ g^{-1}$)	3.39	3.09	5.12	4.57	4.28
	R^2	0.948	0.968	0.952	0.95	0.95

Table 3 Comparison of the prepared AC (AC-100) with other activated carbons

Precursor	Activation conditions	Isotherm model	q_m (mg/g)	Reference
Ficus carica bast fiber	H_3PO_4 Microwave heating (5 min; 600 W)	Langmuir	44.84	[84]
Aloe vera	H_2SO_4, under N_2, 800 °C	Langmuir	58.83	[85]
Watermelon peel	H_2SO_4	Langmuir	72.46	[86]
Silver berry	$ZnCl_2$, 500 °C	Langmuir	88.57	[35]
Orange peel	$ZnCl_2$,700 °C	Langmuir	133.33	[87]
Ficus carica leaves	H_3PO_4, under N_2, 600 °C	Langmuir	155.27	This study
Corn straw	KOH, under N_2, 800 °C	Langmuir	176.37	[88]
Spent coffee grounds	KOH, 400 °C	Langmuir	187.6	[89]

This improvement in AC performance can be attributed to the introduction of new functional groups on the AC surface and an increase in the surface area, resulting in an elevated Cr(VI) adsorption capacity. The results were further corroborated through iodine number, SEM analysis, and FTIR spectra analysis of EDA-AC-100. The iodine number increased from 1270 for AC-100 to 1422 for EDA-AC-100, signifying an augmentation in the microporous surface area.

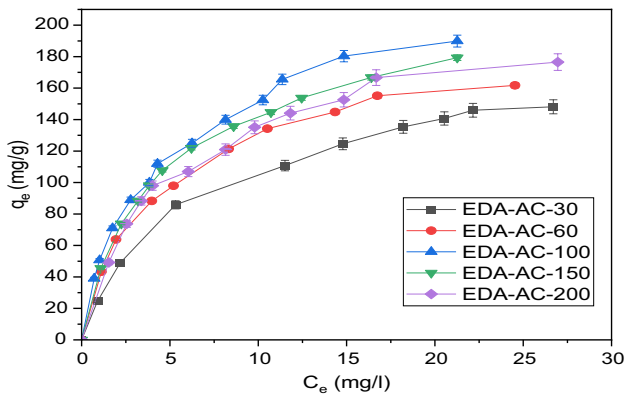

Fig. 12 The isotherms adsorption of the Cr(VI) on the EDA-modified ACs (ACs dose of 2 g/L, pH of 2, a contact time of 2 h, and ambient temperature)

In Fig. 14, the SEM images confirm the enhancement of surface porosity in the modified AC. The FTIR analysis of EDA-AC-100, as shown in Fig. 15, revealed the emergence of new peaks, including one between 1425 and 1375 cm^{-1}, due to the stretching vibration of C(O)-N in amide groups [90], shows the presence of an amidation reaction between AC and EDA. This amidation resulted in the covalent attachment of EDA to AC, characterized by the vibrations of N–H, C-H, and C-N [91]. Another peak appeared at 868 cm^{-1}, indicating the presence of C-N stretching. Additionally, a peak near 3000 cm^{-1} was associated with N–H stretching, and the last peak at 1579 cm^{-1} was possibly related to N–H (amine or amide groups). These peaks provided conclusive evidence of the chemical modification of the prepared AC with EDA. Furthermore, the introduction of new amino groups on the AC surface enhances electrostatic attraction and chelate complex formation with Cr(VI) ions. These results were in agreement with those obtained by [90, 92].

4 Conclusion

In this work, preparation, characterization, and adsorption performances of activated carbons derived from *Ficus carica* leaves for Cr(VI) removal were investigated. The

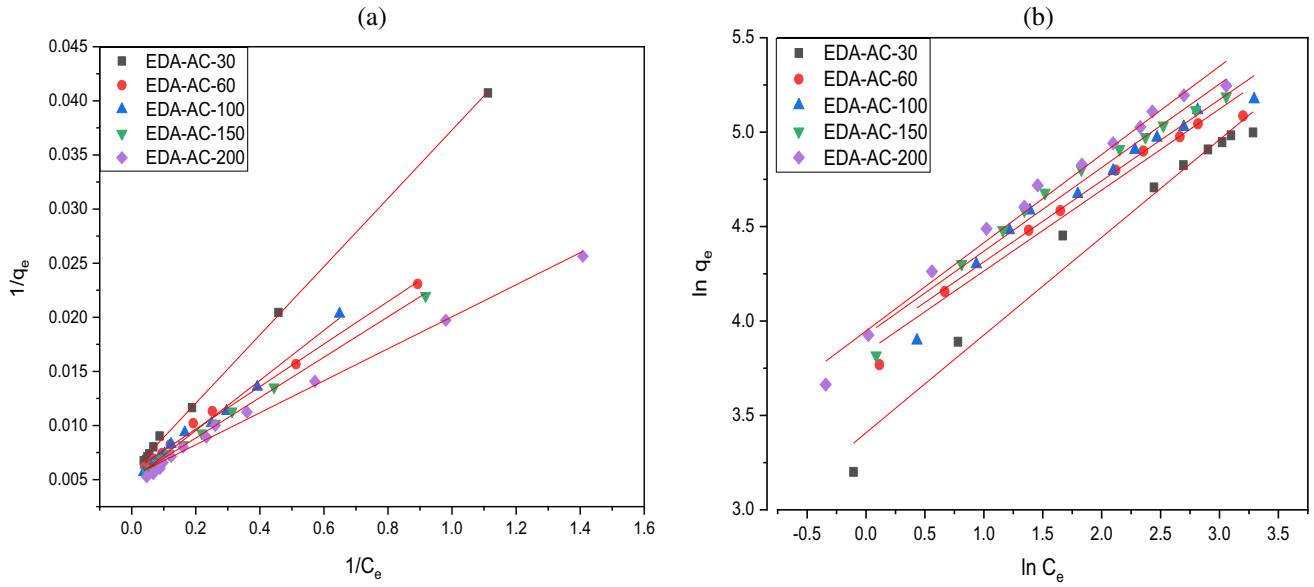

Fig. 13 Linear fit of Langmuir (**a**) and Freundlich (**b**) isotherms models for Cr(VI) removal by the prepared EDA-ACs

Table 4 Adsorption isotherm constants for removal of Cr(VI) using the prepared EDA-ACs

Model	Parameters	Adsorbent				
		EDA-AC-30	EDA-AC-60	EDA-AC-100	EDA-AC-150	EDA-AC-200
Langmuir	q_{max} (mg/g)	173.91	174.52	203.25	195.69	189.75
	K_L (L/mg)	0.18	0.29	0.21	0.27	0.35
	R_L	0.09	0.06	0.08	0.06	0.053
	R^2	0.99	0.99	0.99	0.99	0.992
Freundlich	$1/n$	0.51	0.42	0.42	0.44	0.46
	K_F ($mg^{1-(1/n)}\ L^{1/n}\ g^{-1}$)	30.20	46.27	48.56	50.74	51.77
	R^2	0.97	0.97	0.95	0.96	0.98

prepared ACs (H3PO4, 600 °C, 1 h) were characterized by DRX, SEM–EDS, ATG, FTIR, iodine number, and pH of zero charge. It was found that the prepared ACs have a high microporous surface area and acidic functional groups. The effect of the impregnation ratio of the activating agent (H_3PO_4) and surface modification by ethylenediamine

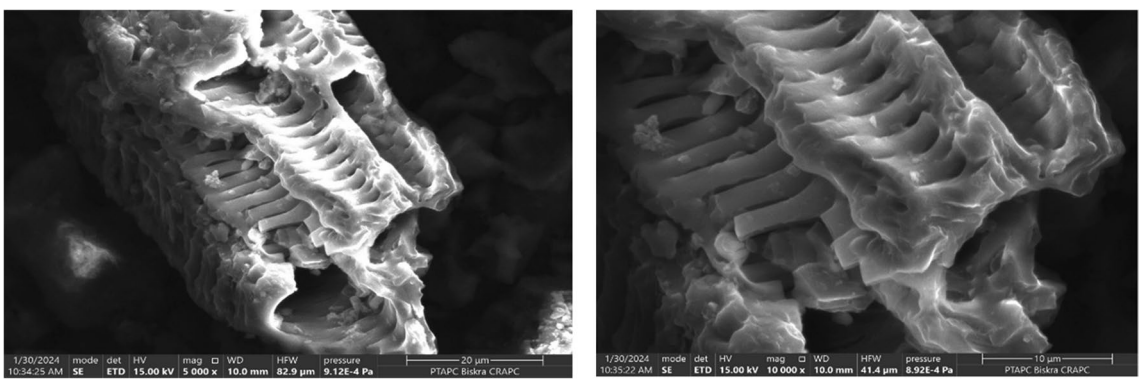

Fig. 14 SEM analysis of EDA-AC-100

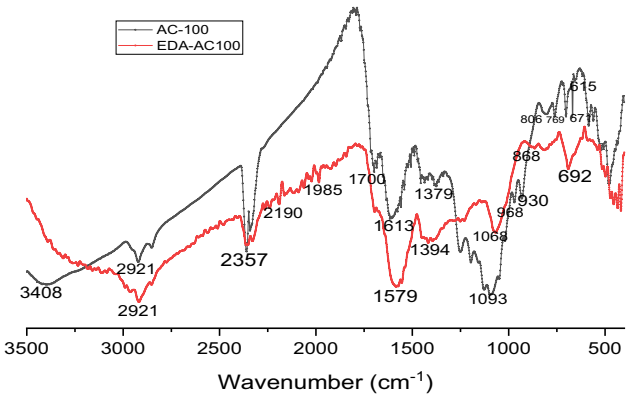

Fig. 15 FTIR spectra of EDA-AC-100 and AC-100

(EDA) was also studied to enhance the ACs performance. Results show that an impregnation ratio of 100% gives the best AC performance, with a maximum capacity adsorption equal to 155.27 mg/g evaluated using Langmuir isotherm under optimal operational conditions such as ACs dose of 2 g/L, pH of 2, and a contact time of 2 h. Results of ACs surface modification show a significant improvement in the adsorption capacity of the produced ACs; the maximum adsorption capacity of Cr(VI) increases from 155.27 to 203.25 mg/g for unmodified and EDA-modified AC-100. Moreover, iodine number, SEM images, and FTIR spectra analysis have successfully confirmed the surface modifications. The introduction of amino groups via EDA not only enhances the adsorption capacity but also facilitates electrostatic attraction and chelate complex formation with Cr(VI) ions. This approach holds considerable promise for enhancing the adsorption performance of ACs and their usefulness in water treatment and environmental remediation applications.

Acknowledgements The authors would like to acknowledge the Ministry of Higher Education and Scientific Research of Algeria and the Laboratory of Inorganic Materials, Department of Chemistry, Faculty of Sciences, University of M'sila for providing the necessary resources for this study.

Author contribution ZB: experiments, investigation, original draft; FB: methodology, writing—review, validation and general discussion—review and editing; AR: reproducibility of results, writing—review and editing; AB: material characterization, data presentation.

Availability of data and materials Not applicable.

Declarations

Ethical approval Not applicable.

Competing interests The authors declare no competing interests.

References

1. Wu Q, Gao L, Huang M, Mersal GA, Ibrahim MM, El-Bahy ZM et al (2022) Aminated lignin by ultrasonic method with enhanced arsenic (V) adsorption from polluted water. Adv Compos Hybrid Mater 5:1044. https://doi.org/10.1007/s42114-022-00492-5
2. Xie X, Gao H, Luo X, Zhang Y, Qin Z, Ji H (2022) Polyethyleneimine-modified magnetic starch microspheres for Cd (II) adsorption in aqueous solutions. Adv Compos Hybrid Mater 5:2772. https://doi.org/10.1007/s42114-022-00422-5
3. Kim E-B, Imran M, Umar A, Akhtar MS, Ameen S (2022) Indandione oligomer@ graphene oxide functionalized nanocomposites for enhanced and selective detection of trace Cr2+ and Cu2+ ions. Adv Compos Hybrid Mater 5:1582. https://doi.org/10.1007/s42114-022-00428-z
4. Dutta B, Bera S, Bairy G, Shit M, Sinha SKC, Mir MH (2022) Exploitation of a series of Zn (II)-coordination polymers for Pd (II)-detection in aqueous medium ES. Energy Environ 16:74. https://doi.org/10.30919/esee8c651
5. Yin H, Zhong W, Yin M, Kang C, Shi L, Tang H et al (2022) Carboxyl-functionalized poly (arylene ether nitrile)-based rare earth coordination polymer nanofibrous membrane for highly sensitive and selective sensing of Fe3+ ions. Adv Compos Hybrid Mater 5:2031. https://doi.org/10.1007/s42114-022-00547-7
6. Zhitkovich A (2011) Chromium in drinking water: sources, metabolism, and cancer risks. 24: 1617. https://doi.org/10.1021/tx200251t
7. Wang Q, Zhang Y, Li Y, Ren J, Qu G, Wang T et al (2022) Simultaneous Cu-EDTA oxidation decomplexation and Cr (VI) reduction in water by persulfate/formate system: reaction process and mechanisms. Chem Eng J 427:131584. https://doi.org/10.1016/j.cej.2021.131584
8. Dong H, Zhang L, Shao P, Hu Z, Yao Z, Xiao Q et al (2023) A metal-organic framework surrounded with conjugate acid-base pairs for the efficient capture of Cr (VI) via hydrogen bonding over a wide pH range. J Hazard Mater 441:129945. https://doi.org/10.1016/j.jhazmat.2022.129945
9. Wen J, Cheng W, Zhang Y, Zhou Y, Zhang Y, Yang L (2023) Highly efficient removal of Cr (VI) from wastewater using electronegative SA/EGCG@ Ti/SA/PVDF sandwich membrane. J Hazard Mater 459:132073
10. Wuana RA, Okieimen FE (2011) Heavy metals in contaminated soils: a review of sources, chemistry, risks and best available strategies for remediation. Int Sch Res Notices https://doi.org/10.5402/2011/402647
11. El Gaayda J, Rachid Y, Titchou FE, Barra I, Hsini A, Yap P-S et al (2023) Optimizing removal of chromium (VI) ions from water by coagulation process using central composite design: effectiveness of grape seed as a green coagulant. Sep Purif Technol 307:122805. https://doi.org/10.1016/j.seppur.2022.122805
12. Gheju M, Balcu I (2011) Removal of chromium from Cr (VI) polluted wastewaters by reduction with scrap iron and subsequent precipitation of resulted cations. J Hazard Mater 196:131. https://doi.org/10.1016/j.jhazmat.2011.09.002
13. Zhang H, Tian Y, Niu Y, Dong X, Lou H, Zhou H (2022) Lignosulfonate/N-butylaniline hollow microspheres for the removal of Cr (VI): fabrication, adsorption isotherm and kinetics. J Water Process Eng 46:102588. https://doi.org/10.1016/j.jwpe.2022.102588
14. Rezvani M, Asgharinezhad AA, Ebrahimzadeh H, Shekari N (2014) A polyaniline-magnetite nanocomposite as an anion exchange sorbent for solid-phase extraction of chromium (VI) ions. Microchim Acta 181:1887. https://doi.org/10.1007/s00604-014-1262-1

15. Çimen A (2015) Removal of chromium from wastewater by reverse osmosis. Russ J Phys Chem 89:1238. https://doi.org/10.1134/S0036024415070055
16. Xiong J, Hu Q, Wu J, Jia Z, Ge S, Cao Y et al (2023) Structurally stable electrospun nanofibrous cellulose acetate/chitosan biocomposite membranes for the removal of chromium ions from the polluted water. Adv Compos Hybrid Mater 6:1. https://doi.org/10.1007/s42114-023-00680-x
17. Meneses IP, Novaes SD, Dezotti RS, Oliveira PV, Petri DFS (2022) CTAB-modified carboxymethyl cellulose/bagasse cryogels for the efficient removal of bisphenol A, methylene blue and Cr (VI) ions: batch and column adsorption studies. J Hazard Mater 421:126804. https://doi.org/10.1016/j.jhazmat.2021.126804
18. Tahir S, Naseem R (2007) Removal of Cr (III) from tannery wastewater by adsorption onto bentonite clay. Sep Purif Technol 53:312. https://doi.org/10.1016/j.seppur.2006.08.008
19. Mohammed Ali GA, Barhoum A, Gupta VK, Nada AA, El-Maghrabi HH, Kanthasamy R et al (2020) High surface area mesoporous silica for hydrogen sulfide effective removal. Curr Nanosci 16:226. https://doi.org/10.2174/1573413715666181205122307
20. Hou K, Xu X, Xiang Y, Chen X, Lam SS, Naushad M et al (2023) Rapid uptake of gold ions by sulfonated humic acid modified phenolic resin with high adsorption capacity and selectivity. Adv Compos Hybrid Mater 6:77. https://doi.org/10.1007/s42114-023-00647-y
21. Si Y, Li J, Cui B, Tang D, Yang L, Murugadoss V et al (2022) Janus phenol–formaldehyde resin and periodic mesoporous organic silica nanoadsorbent for the removal of heavy metal ions and organic dyes from polluted water. Adv Compos Hybrid Mater 5:1180. https://doi.org/10.1007/s42114-022-00446-x
22. Zou H, Zhao J, He F, Zhong Z, Huang J, Zheng Y et al (2021) Ball milling biochar iron oxide composites for the removal of chromium (Cr (VI)) from water: performance and mechanisms. J Hazard Mater 413:125252. https://doi.org/10.1016/j.jhazmat.2021.125252
23. Wang C, Liu X, Yang T, Sridhar D, Algadi H, Bin XuB et al (2023) An overview of metal-organic frameworks and their magnetic composites for the removal of pollutants. Sep Purif Technol 320:124144. https://doi.org/10.1016/j.seppur.2023.124144
24. El-Maghrabi HH, Abdelmaged SM, Nada AA, Zahran F, El-Wahab SA, Yahea D et al (2017) Magnetic graphene based nanocomposite for uranium scavenging. J Hazard Mater 322:370. https://doi.org/10.1016/j.jhazmat.2016.10.007
25. Bhat P, Jain N, Naik N, Samrot AV, Salmataj S (2023) Adsorptive removal of chromium from simulated industrial wastewater using jungle geranium-derived biosorbents. ES Mater Manuf 22:1070. https://doi.org/10.30919/esmm1070
26. Douara N, Benzekri Benallou M, Termoul M, Mekibes Z, Bestani B, Benderdouche N (2022) Removal of textile dyes on a biosorbent based on the leaves of Atriplex halimus. Iran J Chem Chem Eng 41:3726. https://doi.org/10.30492/IJCCE.2022.535090.4864
27. Wang H, Xu J, Liu X, Sheng L (2021) Preparation of straw activated carbon and its application in wastewater treatment: a review. J Clean Prod 283:124671. https://doi.org/10.1016/j.jclepro.2020.124671
28. Mekibes Z, Bestani B, Douara N, Benderdouche N, Benzekri-Benallou M (2021) Simultaneous activation of Ficus carica L. leaves for the removal of emerging pollutants from aqueous solutions Desalin. Water Treat 222:322. https://doi.org/10.5004/dwt.2021.27085
29. Peng J, Kang X, Zhao S, Yin Y, Zhao P, Ragauskas AJ et al (2023) Regulating the properties of activated carbon for supercapacitors: impact of particle size and degree of aromatization of hydrochar. Adv Compos Hybrid Mater 6:1. https://doi.org/10.1007/s42114-023-00682-9
30. Chen X, Zhao S, Kang X, He C, Zhao P, Meng X et al (2023) Gradient synthesis of carbon quantum dots and activated carbon from pulp black liquor for photocatalytic hydrogen evolution and supercapacitor. Adv Compos Hybrid Mater 6:131. https://doi.org/10.1007/s42114-023-00714-4
31. Zhou K, Sheng Y, Guo W, Wu L, Wu H, Hu X et al (2023) Biomass porous carbon/polyethylene glycol shape-stable phase change composites for multi-source driven thermal energy conversion and storage. Adv Compos Hybrid Mater 6:34. https://doi.org/10.1007/s42114-022-00620-1
32. Foo K, Hameed B (2009) Utilization of biodiesel waste as a renewable resource for activated carbon: application to environmental problems. Renew Sustain Energy Rev 13:2495. https://doi.org/10.1016/j.rser.2009.06.009
33. Vozniakovskii A, Kidalov S, Vozniakovskii A, Karmanov A, Kocheva L, Rachkova N (2020) Carbon nanomaterials based on plant biopolymers as radionuclides sorbent Fuller. Nanotub Car N 28:238. https://doi.org/10.1080/1536383X.2019.1686627
34. Acharya J, Sahu J, Sahoo B, Mohanty C, Meikap B (2009) Removal of chromium (VI) from wastewater by activated carbon developed from Tamarind wood activated with zinc chloride. Chem Eng J 150:25. https://doi.org/10.1016/j.cej.2008.11.035
35. Benmahdi F, Khettaf S, Kolli M (2022) Efficient removal of Cr (VI) from aqueous solution using activated carbon synthesized from silver berry seeds: modeling and optimization using central composite design. Biomass Convers Biorefin: 1. https://doi.org/10.1007/s13399-022-03041-8
36. Srivastava A, Gupta B, Majumder A, Gupta AK, Nimbhorkar SK (2021) A comprehensive review on the synthesis, performance, modifications, and regeneration of activated carbon for the adsorptive removal of various water pollutants. J Environ Chem Eng 9:106177. https://doi.org/10.1016/j.jece.2021.106177
37. Sultana M, Rownok MH, Sabrin M, Rahaman MH, Alam SN (2022) A review on experimental chemically modified activated carbon to enhance dye and heavy metals adsorption. Clean Eng Technol 6:100382. https://doi.org/10.1016/j.clet.2021.100382
38. Xiong C, Xiong Q, Zhao M, Wang B, Dai L, Ni Y (2023) Recent advances in non-biomass and biomass-based electromagnetic shielding materials. Adv Compos Hybrid Mater 6:205. https://doi.org/10.1007/s42114-023-00774-6
39. Liang Q, Liu Y, Chen M, Ma L, Yang B, Li L et al (2020) Optimized preparation of activated carbon from coconut shell and municipal sludge. Mater Chem Phys 241:122327. https://doi.org/10.1016/j.matchemphys.2019.122327
40. Han Y, Wang Y, Zhao B, Bai Y, Han S, Zhang Y et al (2023) Carbon dots: building a robust optical shield for wood preservation. Adv Compos Hybrid Mater 6:39. https://doi.org/10.1007/s42114-022-00619-8
41. Wafaa Y, Akazdam S, Zyade S, Chafiq M, Ko YG, Chafi M et al (2023) Mechanistic insights into methylene blue removal via olive stone-activated carbon: a study on surface porosity and characterization. J Saudi Chem Soc 27:101692. https://doi.org/10.1016/j.jscs.2023.101692
42. Benmahdi F, Oulmi K, Khettaf S, Kolli M, Merdrignac-Conanec O, Mandin P (2021) Synthesis and characterization of microporous granular activated carbon from silver berry seeds using ZnCl2 activation. Fuller Nanotub Car N 29:657. https://doi.org/10.1080/1536383X.2021.1878154
43. Keerthanan S, Bhatnagar A, Mahatantila K, Jayasinghe C, Ok YS, Vithanage M (2020) Engineered tea-waste biochar for the removal of caffeine, a model compound in pharmaceuticals and personal care products (PPCPs), from aqueous media. Environ Technol Innov 19:100847. https://doi.org/10.1016/j.eti.2020.100847
44. Jabar JM, Odusote YA, Ayinde YT, Yılmaz M (2022) African almond (Terminalia catappa L) leaves biochar prepared through pyrolysis using H3PO4 as chemical activator for sequestration of methylene blue dye. Results Eng 14:100385. https://doi.org/10.1016/j.rineng.2022.100385
45. Ramutshatsha-Makhwedzha D, Mbaya R, Mavhungu ML (2022) Application of activated carbon banana peel coated with

al2o3-chitosan for the adsorptive removal of lead and cadmium from wastewater. Materials 15:860. https://doi.org/10.3390/ma15030860
46. Shankar P, Thandapani G, Kumar V, Parappurath Narayanan S (2022) Evaluation of batch and packed bed adsorption column for chromium (VI) ion removal from aqueous solution using chitosan-silica–g–AM/orange peel hydrogel composite. Biomass Convers Biorefin: 1. https://doi.org/10.1007/s13399-022-02450-z
47. Fu K, Yue Q, Gao B, Wang Y, Li Q (2017) Activated carbon from tomato stem by chemical activation with FeCl2. Colloids Surf A: Physicochem Eng 529:842. https://doi.org/10.1016/j.colsurfa.2017.06.064
48. Adan-Mas A, Alcaraz L, Arévalo-Cid P, López-Gómez FA, Montemor F (2021) Coffee-derived activated carbon from second biowaste for supercapacitor applications. Waste Manage 120:280. https://doi.org/10.1016/j.wasman.2020.11.043
49. Douara N, Bestani B, Benderdouche N, Duclaux L (2016) Sawdust-based activated carbon ability in the removal of phenol-based organics from aqueous media. Desalin Water Treat 57:5529. https://doi.org/10.1080/19443994.2015.1005151
50. Sun Z, Zhang Y, Guo S, Shi J, Shi C, Qu K et al (2022) Confining FeNi nanoparticles in biomass-derived carbon for effectively photo-Fenton catalytic reaction for polluted water treatment. Adv Compos Hybrid Mater 5:1566. https://doi.org/10.1007/s42114-022-00477-4
51. Medhat A, El-Maghrabi HH, Abdelghany A, Abdel Menem NM, Raynaud P, Moustafa YM et al (2021) Efficiently activated carbons from corn cob for methylene blue adsorption. Appl Surf Sci Adv 3:100037. https://doi.org/10.1016/j.apsadv.2020.100037
52. Tian Y, Zhong L, Sheng X, Zhang X (2022) Corrosion inhibition property and promotion of green basil leaves extract materials on Ti-Zr conversion composite coatings. Adv Compos Hybrid Mater 5:1922. https://doi.org/10.1007/s42114-022-00523-1
53. Scaffaro R, Maio A, Gammino M (2022) Hybrid biocomposites based on polylactic acid and natural fillers from Chamaerops humilis dwarf palm and Posidonia oceanica leaves. Adv Compos Hybrid Mater 5:1988. https://doi.org/10.1007/s42114-022-00534-y
54. Hossain MA, Akhter S, Sohrab MH, Afroz F, Begum MN, Rony SR (2023) Applying an optimization technique for the extraction of antioxidant components from Justicia adhatoda leaves. Eng Sci 24:913. https://doi.org/10.30919/es913
55. Zhao K, Wu X, Han G, Sun L, Zheng C, Hou H et al (2024) Phyllostachys nigra (Lodd. ex Lindl.) derived polysaccharide with enhanced glycolipid metabolism regulation and mice gut microbiome. Int J Biol Macromol 257:128588. https://doi.org/10.1016/j.ijbiomac.2023.128588
56. González-García P (2018) Activated carbon from lignocellulosics precursors: a review of the synthesis methods, characterization techniques and applications. Renew Sustain Energy Rev 82:1393. https://doi.org/10.1016/j.rser.2017.04.117
57. Lozano-Castello D, Lillo-Ródenas M, Cazorla-Amorós D, Linares-Solano A (2001) Preparation of activated carbons from Spanish anthracite: I. Activation by KOH Carbon 39:741. https://doi.org/10.1016/S0008-6223(00)00185-8
58. Raji Y, Nadi A, Mechnou I, Saadouni M, Cherkaoui O, Zyade S (2023) High adsorption capacities of crystal violet dye by low-cost activated carbon prepared from Moroccan Moringa oleifera wastes: characterization, adsorption and mechanism study. Diam Relat Mater 135:109834. https://doi.org/10.1016/j.diamond.2023.109834
59. Ismail IS, Rashidi NA, Yusup S (2022) Production and characterization of bamboo-based activated carbon through single-step H3PO4 activation for CO2 capture. Environ Sci Pollut Res 29:12434. https://doi.org/10.1007/s11356-021-15030-x
60. Baytar O, Ceyhan AA, Şahin Ö (2021) Production of activated carbon from Elaeagnus angustifolia seeds using H3PO4 activator and methylene blue and malachite green adsorption. Int J Phytoremediation 23:693. https://doi.org/10.1080/15226514.2020.1849015
61. Boehm HP (1966) Chemical identification of surface groups. Adv Catal 16:179. https://doi.org/10.1016/S0360-0564(08)60354-5
62. Tan W-F, Lu S-J, Liu F, Feng X-H, He J-Z, Koopal LK (2008) Determination of the point-of-zero charge of manganese oxides with different methods including an improved salt titration method 173:277
63. Gundogdu A, Duran C, Senturk HB, Soylak M, Imamoglu M, Onal Y (2013) Physicochemical characteristics of a novel activated carbon produced from tea industry waste. J Anal Appl Pyrolysis 104:249. https://doi.org/10.1016/j.jaap.2013.07.008
64. D4607–14 A (2006) ASTM standard test method for determination of iodine number of activated carbon 1. West Conshohocken, PA, USA, p. 5
65. Naeini AH, Kalaee M, Moradi O, Khajavi R, Abdouss M (2022) Synthesis, characterization and application of carboxylmethyl cellulose, guar gam, and graphene oxide as novel composite adsorbents for removal of malachite green from aqueous solution. Adv Compos Hybrid Mater. https://doi.org/10.1007/s42114-021-00388-w
66. Boumaraf R, Khettaf S, Benmahdi F, Bouzzafa M, Bouhidel K-E, Bouhelassa M (2022) Removal of the neutral dissolved organic matter from surface waters by activated carbon. Arab J Geosci 15:151. https://doi.org/10.1007/s12517-021-09401-4
67. Ioannidou OA, Zabaniotou AA, Stavropoulos GG, Islam MA, Albanis TA (2010) Preparation of activated carbons from agricultural residues for pesticide adsorption. Chemosphere 80:1328. https://doi.org/10.1016/j.chemosphere.2010.06.044
68. Beltrame KK, Cazetta AL, de Souza PS, Spessato L, Silva TL, Almeida VC (2018) Adsorption of caffeine on mesoporous activated carbon fibers prepared from pineapple plant leaves. Ecotoxicol Environ Saf 147:64. https://doi.org/10.1016/j.ecoenv.2017.08.034
69. Bohli T, Ouederni A, Fiol N, Villaescusa I (2015) Evaluation of an activated carbon from olive stones used as an adsorbent for heavy metal removal from aqueous phases. C R Chim 18:88. https://doi.org/10.1016/j.crci.2014.05.009
70. Bouchelta C, Medjram MS, Bertrand O, Bellat J-P (2008) Preparation and characterization of activated carbon from date stones by physical activation with steam. J Anal Appl Pyrolysis 82:70. https://doi.org/10.1016/j.jaap.2007.12.009
71. Benmahdi F, Semra S, Kolli M, Bouhelassa M (2020) An experimental study of dispersion of an interactive tracer in chemically heterogeneous medium at a column scale. Hydrol Process 34:3932. https://doi.org/10.1002/hyp.13854
72. Ma X, Ouyang F (2013) Adsorption properties of biomass-based activated carbon prepared with spent coffee grounds and pomelo skin by phosphoric acid activation. Appl Surf Sci 268:566. https://doi.org/10.1016/j.apsusc.2013.01.009
73. Xu Y, Li W, Xu T, Wang G, Huan W, Si C (2023) Straightforward fabrication of lignin-derived carbon-bridged graphitic carbon nitride for improved visible photocatalysis of tetracycline hydrochloride assisted by peroxymonosulfate activation. Adv Compos Hybrid Mater 6:197. https://doi.org/10.1007/s42114-023-00779-1
74. Shi Y, Li B, Jiang X, Yu C, Li T, Sun H et al (2023) In situ enhancing thermal and mechanical properties of novel green WPAI nanocomposite membrane via artificially cultivated biomass-based diatom frustules. Adv Compos Hybrid Mater 6:36. https://doi.org/10.1007/s42114-022-00621-0
75. Rehan M, Nada AA, Khattab TA, Abdelwahed NAM, El-Kheir AAA (2020) Development of multifunctional polyacrylonitrile/silver nanocomposite films: antimicrobial activity, catalytic activity, electrical conductivity, UV protection and SERS-active sensor. J Mater Res Technol 9:9380. https://doi.org/10.1016/j.jmrt.2020.05.079
76. Nada AA, Bekheet MF, Roualdes S, Gurlo A, Ayral A (2019) Functionalization of MCM-41 with titanium oxynitride deposited

via PECVD for enhanced removal of methylene blue. J Mol Liq 274:505. https://doi.org/10.1016/j.molliq.2018.10.154
77. Guo Y, Rockstraw DA (2006) Physical and chemical properties of carbons synthesized from xylan, cellulose, and Kraft lignin by H3PO4 activation. Carbon 44:1464. https://doi.org/10.1016/j.carbon.2005.12.002
78. Kouadio L, Koffi C, Diarra M, Kouyaté A, Yapi H, Akesse V et al (2019) Préparation et caractérisation de charbon actif issu de la coque de cacao 7:920
79. Ozdemir I, Şahin M, Orhan R, Erdem M (2014) Preparation and characterization of activated carbon from grape stalk by zinc chloride activation. Fuel Process Technol 125:200. https://doi.org/10.1016/j.fuproc.2014.04.002
80. Li F, Bi Z, Kimura H, Li H, Liu L, Xie X et al (2023) Energy- and cost-efficient salt-assisted synthesis of nitrogen-doped porous carbon matrix decorated with nickel nanoparticles for superior electromagnetic wave absorption. Adv Compos Hybrid Mater 6:133. https://doi.org/10.1007/s42114-023-00710-8
81. Ghorbani F, Kamari S, Zamani S, Akbari S, Salehi M (2020) Optimization and modeling of aqueous Cr (VI) adsorption onto activated carbon prepared from sugar beet bagasse agricultural waste by application of response surface methodology. 18: 100444 https://doi.org/10.1016/j.surfin.2020.100444
82. Freundlich HMF (1906) Over the adsorption in solution. J Phys chem 57:1100–1107
83. Langmuir I (1916) The constitution and fundamental properties of solids and liquids. Part. I Solids. J Am Chem Soc 38:2221. https://doi.org/10.1021/ja02268a002
84. Gupta VK, Pathania D, Sharma S, Singh P (2013) Preparation of bio-based porous carbon by microwave assisted phosphoric acid activation and its use for adsorption of Cr (VI). J Colloid Interface Sci 401:125. https://doi.org/10.1016/j.jcis.2013.03.020
85. Prajapati AK, Das S, Mondal MK (2020) Exhaustive studies on toxic Cr (VI) removal mechanism from aqueous solution using activated carbon of aloe vera waste leaves. J Mol Liq 307:112956. https://doi.org/10.1016/j.molliq.2020.112956
86. El Nemr A (2009) Potential of pomegranate husk carbon for Cr (VI) removal from wastewater: kinetic and isotherm studies. J Hazard Matter 161:132. https://doi.org/10.1016/j.jhazmat.2008.03.093
87. El Nemr A, Aboughaly RM, El Sikaily A, Ragab S, Masoud MS, Ramadan MS (2020) Microporous nano-activated carbon type I derived from orange peel and its application for Cr (VI) removal from aquatic environment. Biomass Convers Biorefin: 1. https://doi.org/10.1007/s13399-020-00995-5.
88. Ma H, Yang J, Gao X, Liu Z, Liu X, Xu Z (2019) Removal of chromium (VI) from water by porous carbon derived from corn straw: influencing factors, regeneration and mechanism. J Hazard Mater 369:550. https://doi.org/10.1016/j.jhazmat.2019.02.063
89. Loulidi I, Jabri M, Amar A, Kali A, Alrashdi AA, Hadey C et al (2023) Comparative study on adsorption of crystal violet and chromium (VI) by activated carbon derived from spent coffee grounds. Appl Sci 13:985. https://doi.org/10.3390/app13020985
90. Fu X, Yang H, Sun H, Lu G, Wu J (2016) The multiple roles of ethylenediamine modification at TiO2/activated carbon in determining adsorption and visible-light-driven photoreduction of aqueous Cr (VI). J Alloys Compd 662:165. https://doi.org/10.1016/j.jallcom.2015.12.019
91. Georgiev A, Karamancheva I, Dimov D, Zhivkov I, Spassova E (2008) FTIR study of the structures of vapor deposited PMDA–ODA film in presence of copper phthalocyanine. J Mol Struct 888:214. https://doi.org/10.1016/j.molstruc.2007.12.006
92. Zhu J, Yang J, Deng B (2010) Ethylenediamine-modified activated carbon for aqueous lead adsorption. Environ Chem Lett 8:277. https://doi.org/10.1007/s10311-009-0217-y